NH_3 Sorption Isotherms in ALPO-11 and Its Si, Co, and Mn Analogues

Puyam S. Singh,[†] Praphulla N. Joshi, Subhash P. Mirajkar, Bollapragada S. Rao, and Vasudeo P. Shiralkar*

Catalysis Division, National Chemical Laboratory, Pune - 411008, India

Received: March 16, 1999

Equilibrium sorption capacities of different probe molecules such as water, *n*-hexane, cyclohexane, and ammonia were used as a tool for the characterization of ALPO-11 and protonic forms of SAPO-11, CoAPO-11, and MnAPO-11. Sorption uptake at $P/P_0 = 0.8$ and 298 K, 2 h for water, *n*-hexane, and cyclohexane was found to be affected by incorporating Si, Co, and Mn in ALPO-11. Generation of Bronsted acidity is expected to increase the hydrophilicity; Si, Co, and Mn analogues have exhibited such trends depending upon the extent of substitution and characteristics of the substituted cation. The amount of ammonia retained irreversibly (on account of chemisorption) during sorption measurements was found to be correlated with the intrinsic acidity possessed by ALPO-11 and its analogues. Isotherms of ammonia sorption in ALPO-11, SAPO-11, CoAPO-11, and MnAPO-11 in the temperature range 333−483 K up to 500 Torr have been measured. The NH_3 sorption capacity was also found to decrease in the order ALPO-11 > SAPO-11 > CoAPO-11 > MnAPO-11. The sorption data were analyzed in terms of different models of sorption isotherm equations. BET, Dubinin, Langmuir, and Freundlich isotherm models could represent the sorption data satisfactorily yielding linear plots. However, Sips equation failed to represent ammonia sorption data in these phosphate-containing molecular sieves. At constant coverage, the isosteric heat values have shown the major contribution due to sorbate−sorbent interactions irrespective of the chemical composition.

1. Introduction

Recent developments in the area of solid acid catalysts have brought about many novel phosphate-containing molecular sieves, for which no natural counterparts exist. The hydrothermal synthesis for one such member, AEL-type molecular sieve, was first desrcibed in U.S. Patent applications.[1] The disclosed framework topology[2] of ALPO-11 confirms an orthorhombic structure having a 10-ring channel system bound by 4.1 × 7.0 Å. The substituted aluminophosphates, on account of their typical framework structure and the acidic and redox sites associated with it, are looked upon as a potential industrial catalyst in organic transformation reactions.[3] Usually the acidic as well as sorption properties of zeolites are probed by basic molecules like ammonia, *n*-butylamine, etc. The former, being comparatively smaller and more polar, is probably considered to be best suited for this purpose. With the exception of a few reports,[4] the literature does not reveal much work on the sorption properties of AEL-type aluminophosphate molecular sieve. Prompted by this, we measured sorption capacities of water, *n*-hexane, and cyclohexane (298 K) and studied sorption isotherms of ammonia (333−483 K) in ALPO-11 and its Si, Co, and Mn isomorphs.

2. Experimental Section

2.1. Materials. ALPO-11, SAPO-11, CoAPO-11, and MnAPO-11 were prepared by hydrothermal synthesis in accordance with the method described elsewhere.[1,5] The detailed characterization and their catalytic properties have already been reported elsewhere.[6] The chemical composition of the samples was determined by the combination of wet chemical analysis, X-ray fluorescence spectroscopy, and atomic absorption spectroscopy. The ammonia (purity > 99.9%) was further purified by passing it over freshly ignited calcium oxide, potassium hydroxide pellets, and activated molecular sieve. For sorption measurements, double distilled water, *n*-hexane (> 99.9%, Aldrich), and cyclohexane (99.9%, Aldrich) were used in as-supplied form.

TABLE 1. Unit Cell Composition (on Anhydrous Basis) of ALPO-11 and Its Si, Co, and Mn Analogues

sample	unit cell composition	no. of unit cells/g × 10^{-20}
ALPO-11	$Al_{20}P_{20}O_{80}$	2.4704
SAPO-11	$H_{3.2}Si_{3.2}Al_{19.6}P_{17.2}O_{80}$	2.4735
CoAPO-11	$H_{1.4}Co_{1.4}Al_{18.6}P_{20}O_{80}$	2.4232
MnAPO-11	$H_{0.6}Mn_{0.6}Al_{19.4}P_{20}O_{80}$	2.4515

TABLE 2. Sorption Properties of ALPO-11 and Its Si, Co, and Mn Analogues, $P/P_0 = 0.8$, Temperature = 298 K, 2 h

sample	amount sorbed, wt %[a]			hydrophilicity (H_2O/*n*-hexane)
	H_2O	*n*-C_6H_{14}	C_6H_{12}	
ALPO-11	14.58 (19.78)	7.20 (2.04)	5.10 (1.48)	2.025 (9.696)
SAPO-11	17.56 (23.68)	6.83 (1.93)	4.94 (1.43)	2.571 (12.27)
CoAPO-11	11.29 (15.55)	5.43 (1.56)	3.49 (1.03)	2.079 (9.968)
MnAPO-11	11.69 (15.91)	5.40 (1.54)	3.23 (0.94)	2.165 (10.33)

[a] Numbers in parentheses indicate sorption capacity in molecules per unit cell.

2.2. Methods. The adsorption isotherms were obtained by using an all-glass gravimetric unit connected to a high-vacuum system, described earlier.[7] The sorption isotherms were measured up to 500 Torr in the temperture range 333−483 K. The equilibrium pressure was measured using a Baratron pressure

* To whom all correspondence should be addressed. E-mail: vps@cata.ncl.res.in. Fax: 91-20-5893761.

[†] Present Address: Physical and Theoretical Chemistry Department, Research School of Chemistry, Australian National University, Canberra, ACT 0200, Australia.

10.1021/jp990914b CCC: $18.00
Published on Web 06/06/1999

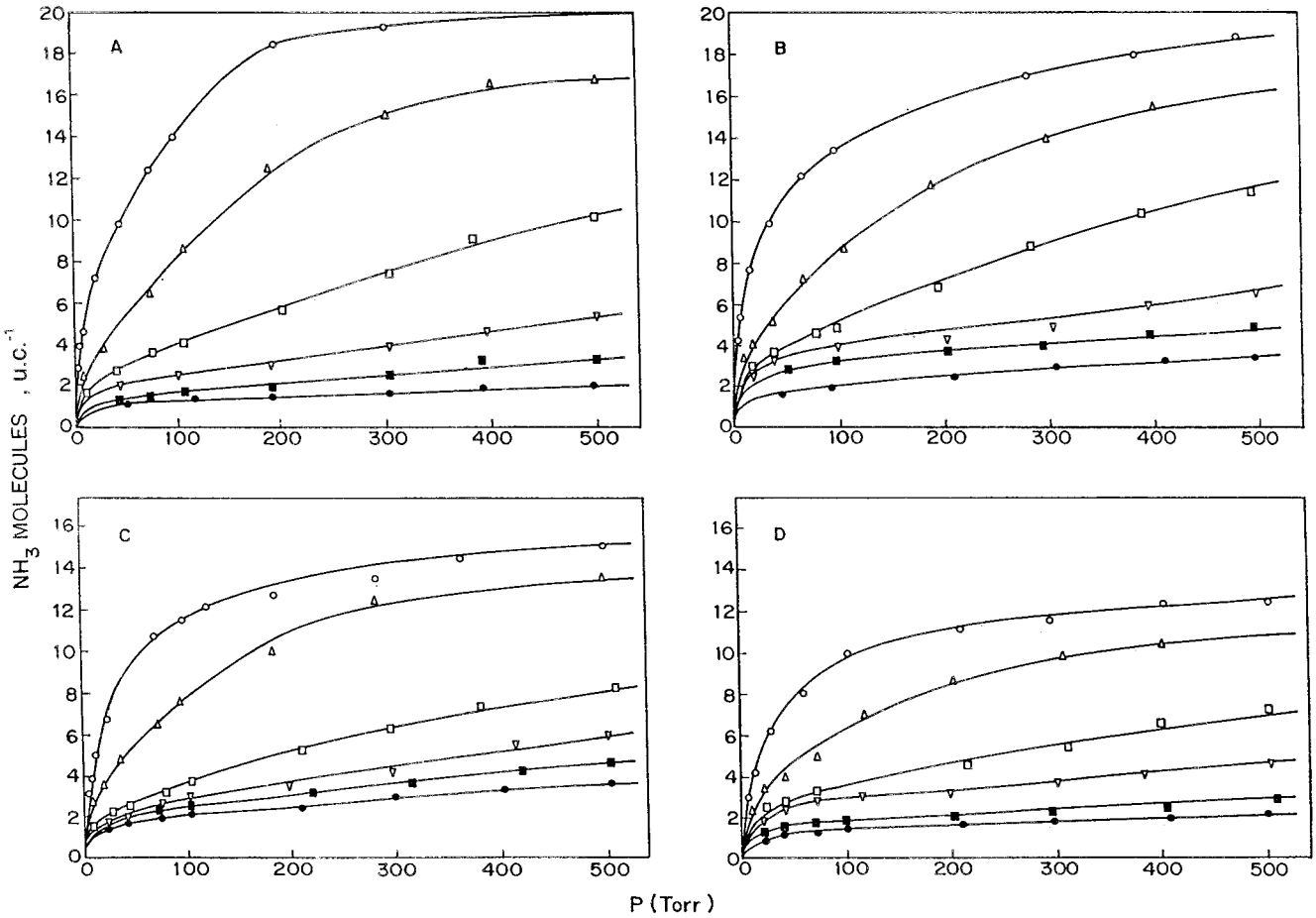

Figure 1. Isotherms for ammonia sorption in (A) $ALPO_4$-11, (B) SAPO-11, (C) CoAPO-11, and (D) MnAPO-11 at (○) 333, (△) 363, (□) 393, (▽) 423, (■) 453, and (●) 483 K.

sensor. The temperature accuracy throughout the sorption experiments was within ±1 K. The sample was degassed at 723 K for 10 h under vacuum, and the temperature was then lowered down to the isotherm temperature, at which it was then allowed to stabilize and was maintained for 2 h before the commencement of the measurement. By adjusting the sorbate pressure, the amount sorbed was measured accurately from the change in the weight of the sample over the time period of 2 h. To check the reversibility of the sorption, desorption measurements were also carried out. After each isotherm, the sample was evacuated at 723 K at 10^{-6} Torr for 10 h. X-ray diffractograms and UV−vis and ESR spectra were recorded for the samples before and after sorption measurements to check the stability, purity, and crystallinity of the AEL phase and the state of Co and Mn cations.

3. Results and Discussion

Unit cell compositions of the four samples used in the present studies are tabulated in Table 1. As reported in our ealier communication,[6] these samples are fully crystalline and contain no extraframework metal cations and have no contribution due to amorphous or dense phase(s). SEM results have shown nearly spherical morphology for all the sample with the crystallite size in the range 1−5 μm.

The UV−vis spectra of the calcined sample of CoAlPO-11, prior to and after the adsorption, showed essentially the same pattern. The intensity of a triplet around 545−640 nm was found unaltered, indicating no conversion from tetrahedral Co^{2+} to Co^{3+}. Similarly, the X band ESR spectra of the calcined dehydrated MnAlPO-11 sample before and after adsorption exhibited no change in hyperfine splitting and the intensity, indicative of the same population of Mn^{2+} species.

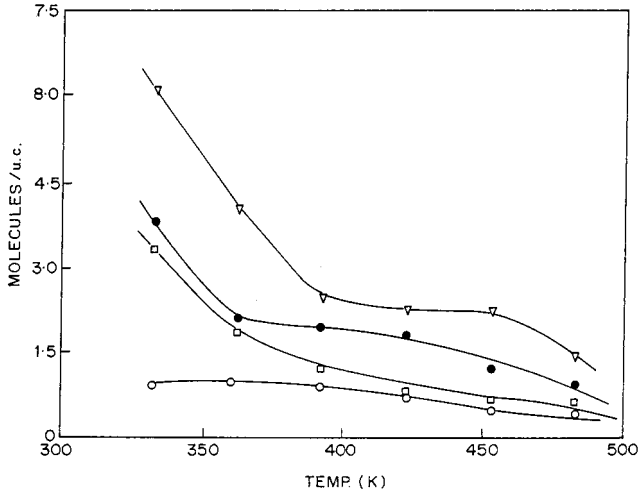

Figure 2. Amount of ammonia molecules held irreversibly as a function of temperature in (▽) CoAPO-11, (●) MnAPO-11, (□) SAPO-11, and (○) $ALPO_4$-11.

3.1. Uptake of Sorbates. Table 2 summarizes sorption uptakes obtained from the measurements at $P/P_0 = 0.8$ and 298 K of different sorbates in AEL-type molecular sieve materials and the hydrophilicity parameter expressed as the ratio H_2O/*n*-hexane. The incorporation of silicon in the framework has been reported for the creation of Bronsted acid sites in the sample which is responsible for the enhanced hydrophilicity.[8] The high packing efficiency of the nonpolar, cylindrical

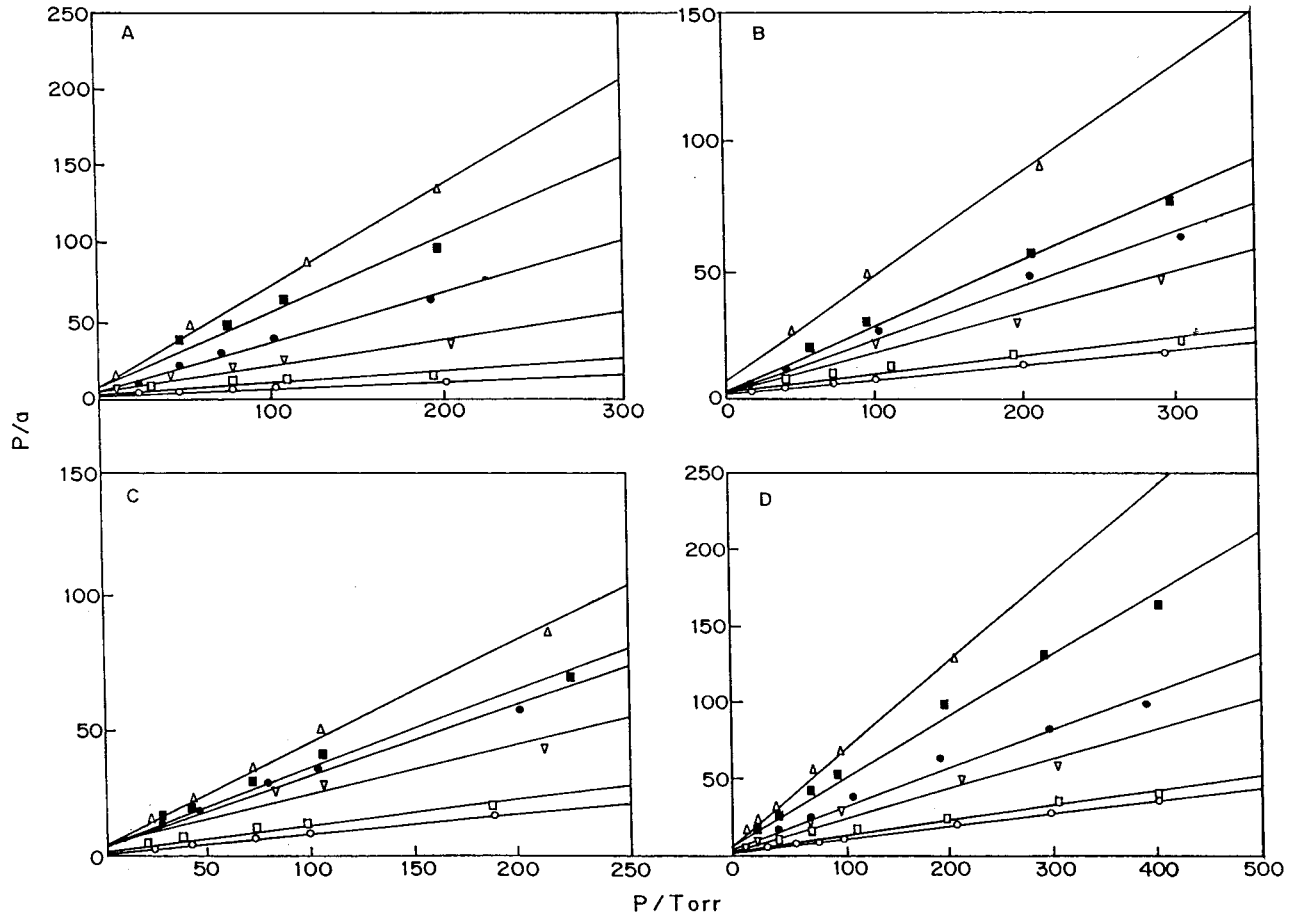

Figure 3. Langmuir plots for ammonia sorption in (A) $ALPO_4$-11, (B) SAPO-11, (C) CoAPO-11, and (D) MnAPO-11 at (△) 483, (■) 453, (●) 423, (▽) 393, (□) 363, and (○) 333 K.

n-hexane molecule (kinetic diameter = 4.2 Å) was expected to yield a more realistic estimate of the void volume. The higher *n*-hexane affinity may also be due to the favorable interactions of a higher number of paraffinic hydrogen atoms with the channel wall. Therefore, the preferential sorption of water over *n*-hexane under the same set of experimental conditions can be taken as a measure of hydrophilicity. The ratio H_2O/*n*-hexane was considered as a criterion to determine the hydrophilicity trend in the present studies. It is seen from the Table 2 that hydrophilicity increases depending on the extent of substitution and the characteristics of the substituent cation.

The equilibrium sorption uptakes of both water and hydrocarbons decrease in the metal-substituted AEL-type aluminophosphate molecular sieve. As reported in the earlier pioneering works, the cycohexane uptake (wt %) is 5.3 for ALPO-11[1a] (measured at 24 °C, 30 Torr), 4.5 for SAPO-11[1b] (measured at 24.6 °C, 52 Torr), 4.0 for VAPO-11[9a] (measured at 24 °C, 90 Torr), and 1.5 for MAPO-11[9b] (measured at 25 °C, 74 Torr). From the above results, it is seen that, despite higher P/P_0, the cyclohexane sorption capacity decreases in Si-, V-, and Mg-substituted AEL-type aluminophosphate framework. Further, a recent report[9c] on chromium-substituted aluminophosphates also reveals that the *n*-butane sorption uptake for CrAPO-11 is 0.07 mL/g and is rather less than that of ALPO-11 (0.08 mL/g). The observed decrease in the above-mentioned sorption capacities of the hydrocarbons may be associated with the combined and complex effects of polarizability, *e*/*r*, packing efficiency of sorbate molecules, the concentration of framework cations, and sorbate−sorbate and sorbate−sorbent interactions and may not be due to the presence of any occluded metal oxide or amorphous materials.

3.2. Isotherms. Families of isotherms of ammonia sorption are presented in Figure 1 for ALPO-11 and Si-, Co-, and Mn-substituted ALPO-11. It can be seen from the figure that the sorption isotherms at lower temperature approximate almost a Langmuir-type or type I isotherm according to Kiselev's classification.[10] Almost 80−90% of the total uptake at 500 Torr takes place within 200 Torr. Except in the very low pressure region (∼20 Torr), the sorption isotherms at higher temperatures (423−483 K) approach Henry's isotherm, showing a linear relationship between equilibrium presurre and amount of ammonia sorbed. The uptake of ammonia is in the following order: MnAPO-11 < CoAPO-11 < SAPO-11 < ALPO-11. A pronounced increase of ammonia uptake in ALPO-11 is due to larger void volume. Factors like Sanderson's electronegativity, polarizability, (*e*/*r*) of the substituted Si or metal, specific surface areas, and void volumes of the framework are expected to influence the sorption capacities and energetics of the sorption of a polar molecule like ammonia.

3.3. Desorption of Ammonia, Irreversibility of Ammonia Sorption, and Acidity. Ammonia, being a molecule that can easily donate a lone pair of electron, interacts strongly with acid sites of the sample. It was found that all the samples studied retained a certain amount of ammonia upon desorption under vacuum (10^{-6} Torr). The phenomenon of irreversibility of ammonia sorption has been reported earlier in MnY,[11] cation exchanged Y,[12] and Ru, Cr, and Fe mordenites[13] at 303 K and is attributed[11] to (a) formation of ammonia complexes with intrazeolite cations and (b) chemisorption. The number of ammonia molecules held (Figure 2) on account of a different degree of chemisorption may be taken as a measure of acidity, whereas physically sorbed ammonia molecules are desorbed by

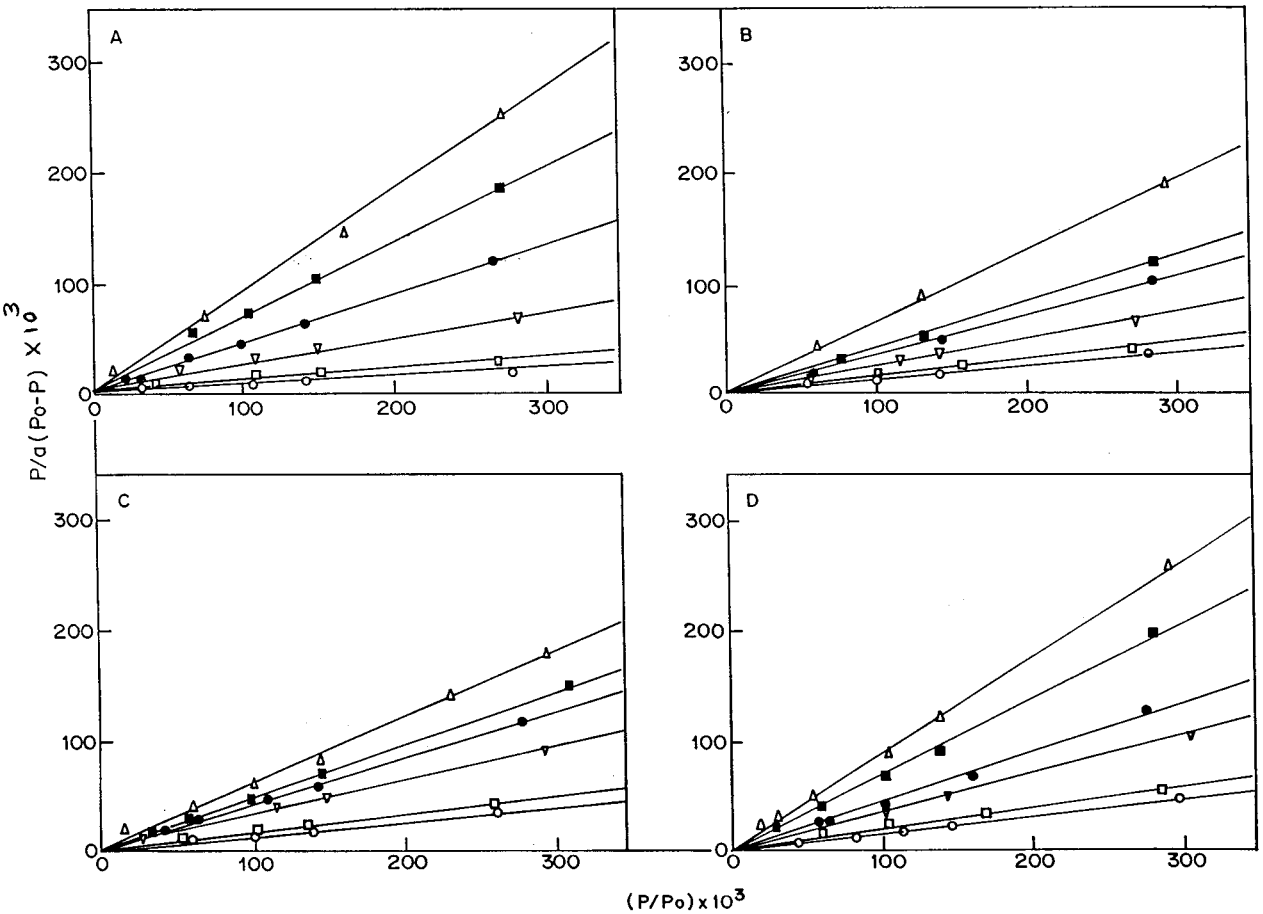

Figure 4. BET plots for ammonia sorption in (A) $ALPO_4$-11, (B) SAPO-11, (C) CoAPO-11, and (D) MnAPO-11 at (△) 483, (■) 453, (●) 423, (▽) 393, (□) 363, and (○) 333 K.

degassing at lower pressure without increasing the temperature. The degree of ammonia retained depends on the interaction of ammonia molecules with the acid centers of the sample. In substituted ALPO-11, the acidity can be generated by various modes, like the terminal hydroxyl group, protons produced from dissociating water molecules by the electrostatic field associated with the extraframework multivalent cations, and Bronsted acid sites. It can be seen from Figure 2 that the amount of ammonia retained decreased at higher temperatures. Although the sorption uptake of ammonia is highest for ALPO-11, the amount of ammonia retained is lowest, indicating that ALPO-11 possesses relatively weaker acid sites. The generation of stronger Bronsted acid sites due to the substitution of Si^{4+} in the ALPO-11 framework causes more ammonia molecules to be strongly chemisorbed over Bronsted acid sites. A substitution of Al^{3+} by Me^{2+} (Me = Co^{2+} or Mn^{2+}) generates much stronger Bronsted acid sites. The electrostatic field associated with the substitution of a more electropositive metal in place of less electropositive aluminum generates stronger negative charge in the framework producing stronger protons. Thus, for metal (Co or Mn) substituted ALPO-11, the ammonia molecules are held strongly on Bronsted acid sites, perhaps on account of chemisorption. Hence, more ammonia molecules are held up in the framework, which are not easily degassed during the desorption experiments.

3.4. Application of Isotherm Equations. *3.4.1. Langmuir Sorption Model.* A Langmuir sorption isotherm equation has been derived on the assumption of localized monolayer sorption on the sorption centers of equal energy and 1:1 correspondence between the sorption centers and sorbate molecules. In the present studies, the ammonia sorption data in different phosphate-containing molecular sieves of AEL type exhibit excellent linear plots, typical examples of which are shown in Figure 3. From Figure 3, it is seen that linear plots are obtained up to 300 Torr, and thereafter, these plots deviate slightly from linearity in the higher pressure region. The salient feature of the linear plots is the increase in the intercept, made by these plots on the ordinate with the increase in the sorption temperature. According to the derivation of this sorption model, the reciprocal of the intercept on the ordinate approximates to the constant "*C*", the heat of sorption of the first layer. Therefore, it seems logical that with the increase in sorption temperature, the heat of sorption decreases as is shown by the reciprocal of the slope of the ordinate. The higher the value of *C*, the stronger is the interaction between the sorption center and the sorbate molecules. The excellent linearity of these plots in Figure 3 undoubtedly shows the validity of the Langmuir equation to describe ammonia sorption in different phosphate-containing molecular sieves. It seems, therefore, that the sorbed ammonia molecules in these phosphate-containing molecular sieves are localized with some contribution of chemisorption indicated by irreversibly retained ammonia discussed earlier. Although *n*-butylamine sorption in EU-1[14] and Fe^{3+}-exchanged Y zeolites[15] yielded linear plots, the Langmuir equation failed to represent CO_2[16] and NH_3[12] sorption in different cation-exchanged Y zeolites.

3.4.2. BET Equation. The BET isotherm equation is based on the assumption of formation of a multilayer with a special and much higher value of heat of sorption for the formation of the first layer than for formation of successive layers. Figure 4 shows a typical example of the linear BET plots obtained from the analysis of ammonia sorption data in different phosphate-containing molecular sieves. All the plots begin from the origin

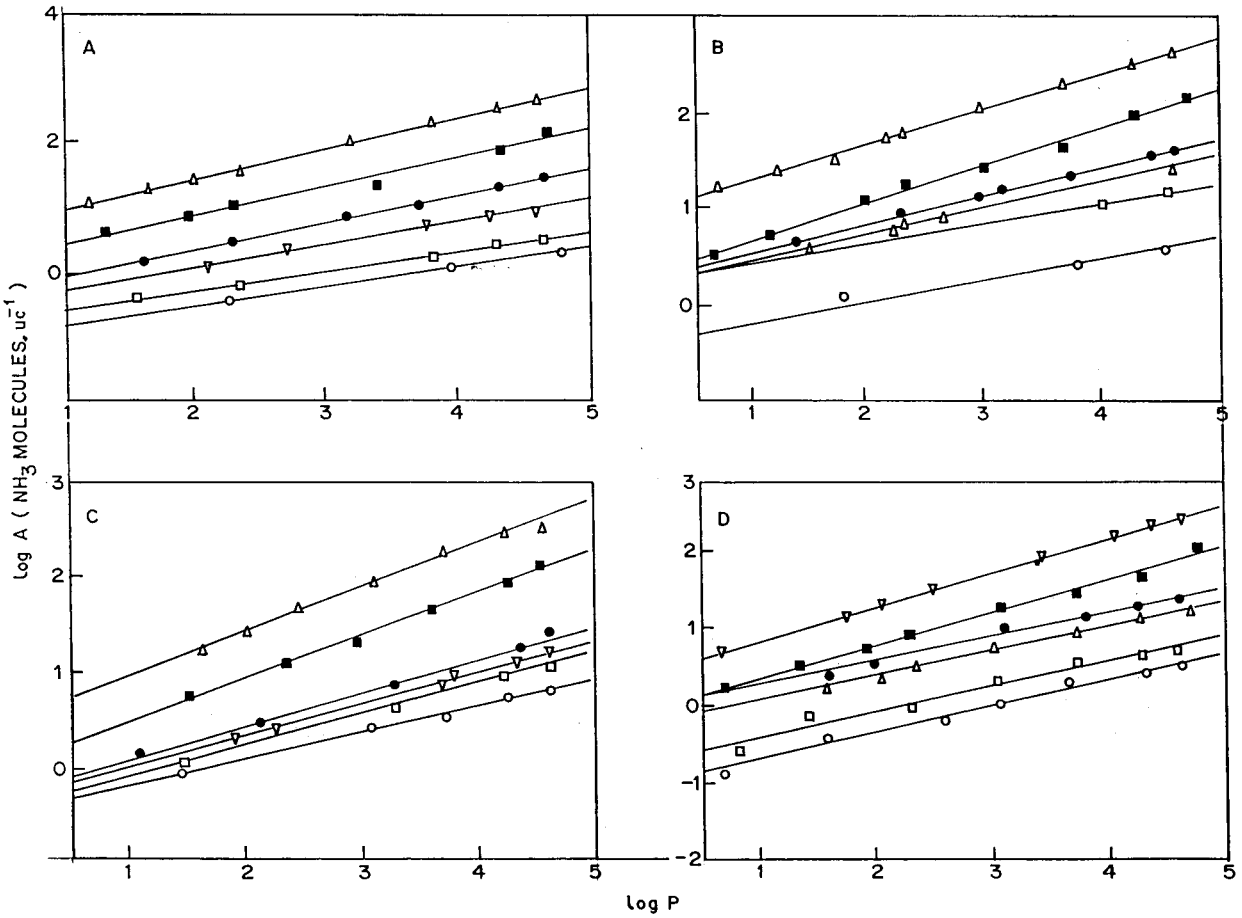

Figure 5. Freundlich plots for ammonia sorption in (A) $ALPO_4$-11, (B) SAPO-11, (C) CoAPO-11, and (D) MnAPO-11 at (△) 333, (■) 363, (●) 393, (▽) 423, (□) 453, and (○) 483 K.

yielding no appreciable intercept on the ordinate even at higher temperature. This indicates a much higher value of the constant *C* in the BET equation. Despite excellent linearity of these BET plots, the monolayer capacities obtained from slopes and intercept of these plots are considerably lower than the experimental ones as well as those obtained from the Langmuir approach. This shows that a BET approach based on the multilayer formation has only a limited applicability in the present studies of ammonia sorption in different phosphate-containing molecular sieves. Perhaps some limitations are expected to be on the multilayer formation on account of the geometry and size of the intracrystalline cages. However, *n*-butylamine sorption data in EU-1[14] zeolites were satisfactorily represented by linear BET plots with monolayer capacities to be in close agreement with those obtained experimentally.

Although assumptionwise the Langmuir equation is based on the monolayer sorption and the BET on the multilayer sorption, if one takes into consideration the limitations most of the zeolite cavities would offer to the formation of more than one layer, essentially the BET equation reduces to the Langmuir equation. If the derivation of the BET sorption isotherm equation is taken into consideration, the first layer of sorbate has a very high (special) value of heat of adsorption compared with that for the successive layers, as far as only the first layer is operative it behaves similarly to the Langmuir equation.

3.4.3. Freundlich Equation. In the lower pressure range, the Langmuir equation takes the special form of the Freundlich equation and the sorbate phase assumes the two-dimensional film on the sorbent surface. Analysis of ammonia sorption data in different phosphate-containing molecular sieves in terms of the Freundlich isotherm model yielded excellent linear plots over the entire coverage in the temperature range 333−483 K. Typical Freundlich plots are shown in Figure 5. The excellent linearity of these plots confirms the applicability of the Freundlich isotherm equation to ammonia sorption in phosphate-containing molecular sieves having AEL topology. *n*-Butylamine sorption data in Al and Fe analogues of beta zeolites,[17] Fe^{3+}-exchanged Y zeolites,[15] and also in different cationic forms of LTL zeolites[18] could satisfactorily be represented by the Freundlich equation, which however, failed to represent *n*-butylamine sorption in EU-1 zeolites.[14]

3.4.4. Dubinin Equation. Polanyi's potential theory when modified by Dubinin and Radushkevich[19] takes the form

$$\log(W) = \log(W_o) - B/2.303\beta^2[T(P_0/P)]^2 \qquad (1)$$

where W is the amount sorbed at equilibrium pressure P, W_o is the total sorption capacity, B is the constant independent of temperature and is a characteristic of the sorbent pore structure, and β is the affinity coefficient.

Usually when the volume-filling phenomenon is operative during the sorption in zeolitic cavities, the surface potential decreases with the progressive filling of the zeolite void and the Dubinin−Radushkevich equation represents the sorption energetics. It is our observation in our previous publications[18a,20] that, in the case of CO_2 and NH_3 sorption in cation-exchanged Y zeolites, if the Dubinin−Radushkevich equation represents the sorption data with fairly linear plots, the Dubinin−Radushkevich characteristic curves show independence of curve $(w) = f(A)$ from the temperature of sorption.

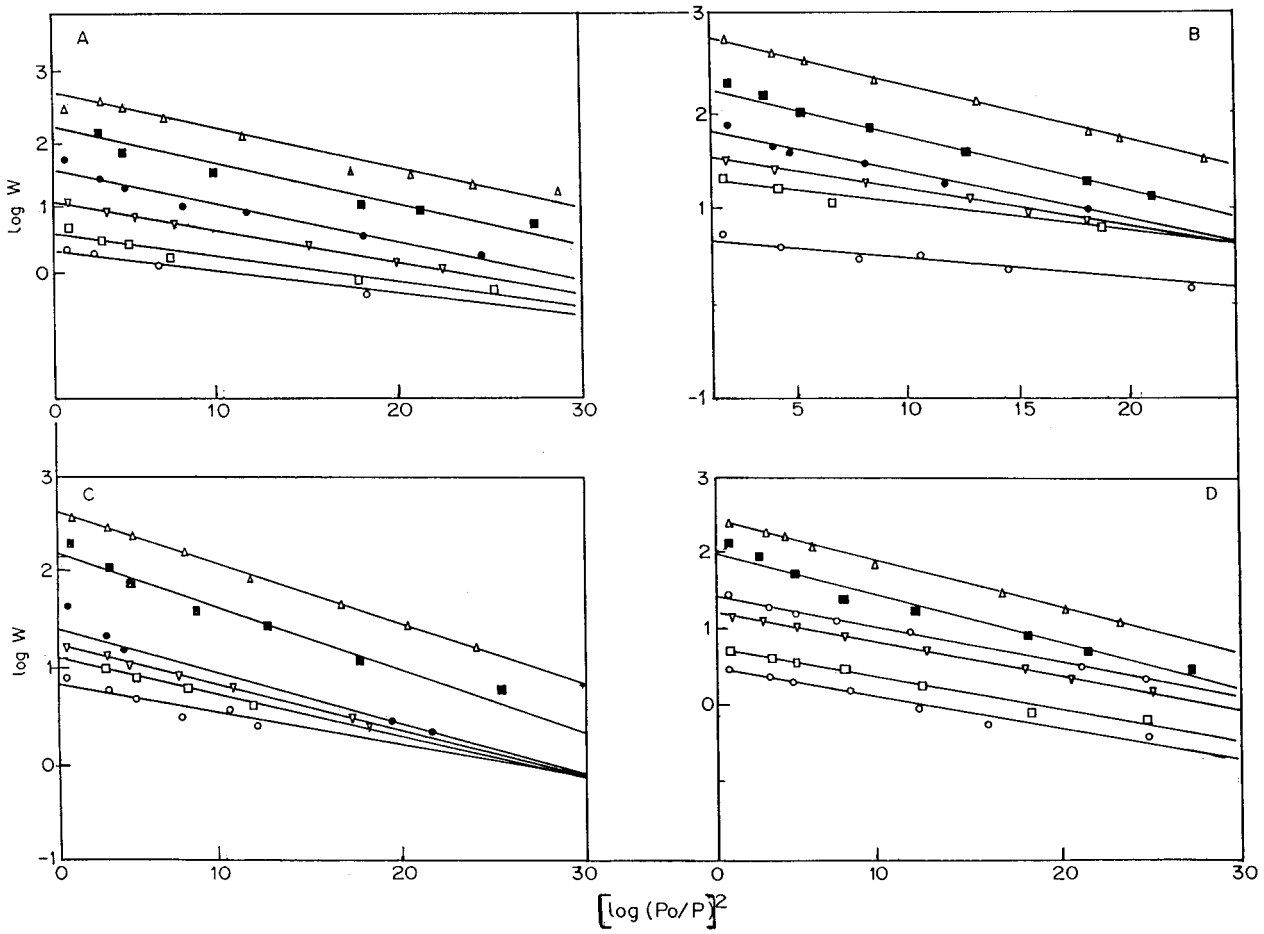

Figure 6. Dubinin plots for ammonia sorption in (A) $ALPO_4$-11, (B) SAPO-11, (C) CoAPO-11, and (D) MnAPO-11 at (△) 333, (■) 363, (●) 393, (▽) 423, (□) 453, and (○) 483 K.

Dubinin plots were constructed by plotting $(\log P_0/P)^2$ against $\log W$ for all the phosphate-containing molecular sieves having AEL topology in the temperature range 333−483 K. In all the samples, excellent linear plots were obtained, and typical Dubinin plots are shown in Figure 6. The saturation capacities (Table 3) obtained from the intercept of these linear plots on the ordinate are comparable with the experimental values within the experimental error.

The slope of these linear Dubinin plots increases marginally with the decrease in sorption temperature. This means B/β^2 (Table 3) decreases with the increase in sorption temperature and, in turn, the affinity coefficient, β, increases with the increase in sorption temperature. An increase or decrease in β may usually be looked upon as an increase or decrease in sorption affinity of a sorbate molecule toward sorption centers on the surface. It is found from Table 3 that the affinity coefficient follows the sequence SAPO-11 > MnAPO-11 > CoAPO-11 > ALPO-11, which seems to bear some relations to the expected acidity induced on the silicon or metal substitution in ALPO-11. This also has been revealed in our present studies, and the experimental data have shown the affinity coefficient followed the sequence SAPO-11 > MnAPO-11 > CoAPO-11 > AlPO-11. The sorption affinity of a sorbate molecule toward sorption centers on the surface at different temperatures may be associated with the increase and/or decrease in β. In general, the excellent linearity of these plots suggests that the ammonia sorption in phosphate-containing molecular sieves, having AEL topology, could satisfactorily be described by the Polanyi potential theory modified by Dubinin and co-workers. CO_2[16] and NH_3[12] sorption data in cation-exchanged Y-type zeolites were also satisfactorily described by Dubinin equation.

TABLE 3. Saturation Capacities and B/β^2 of ALPO-11 and Its Si, Co, and Mn Analogues

	saturation capacities (molecules/unit cell)				
T, K	Langmuir	BET	Dubinin	exptl	$B/\beta^2 \times 10^7$
		ALPO-11			
333	20.49	12.06	17.46	20.22	6.06
363	16.00	9.05	14.28	17.76	5.21
393	5.85	4.33	5.21	7.45	4.14
423	3.10	2.27	3.19	4.72	3.07
453	2.02	1.51	1.93	2.60	2.20
483	1.51	1.09	1.42	1.66	1.90
		SAPO-11			
333	17.15	11.43	16.61	16.89	5.19
363	14.24	8.58	10.12	13.93	4.24
393	6.58	4.87	5.78	8.98	3.13
423	4.88	3.17	4.66	4.94	2.19
453	3.97	2.66	3.63	3.94	1.42
483	2.45	1.69	1.72	3.17	1.32
		CoAPO-11			
333	13.35	9.90	14.58	13.49	5.71
363	10.33	7.53	9.39	11.58	4.93
393	5.29	3.65	4.41	6.27	3.52
423	3.62	2.62	3.56	4.23	2.68
453	3.34	2.28	3.16	3.57	2.21
483	2.51	1.79	2.34	3.08	1.45
		MnAPO-11			
333	12.29	8.26	12.30	12.27	5.64
363	10.64	6.32	7.86	9.43	4.77
393	5.21	3.16	4.44	5.42	3.01
423	3.94	2.43	3.56	3.72	2.51
453	2.48	1.55	2.22	2.51	2.07
483	1.74	1.22	1.73	2.00	1.82

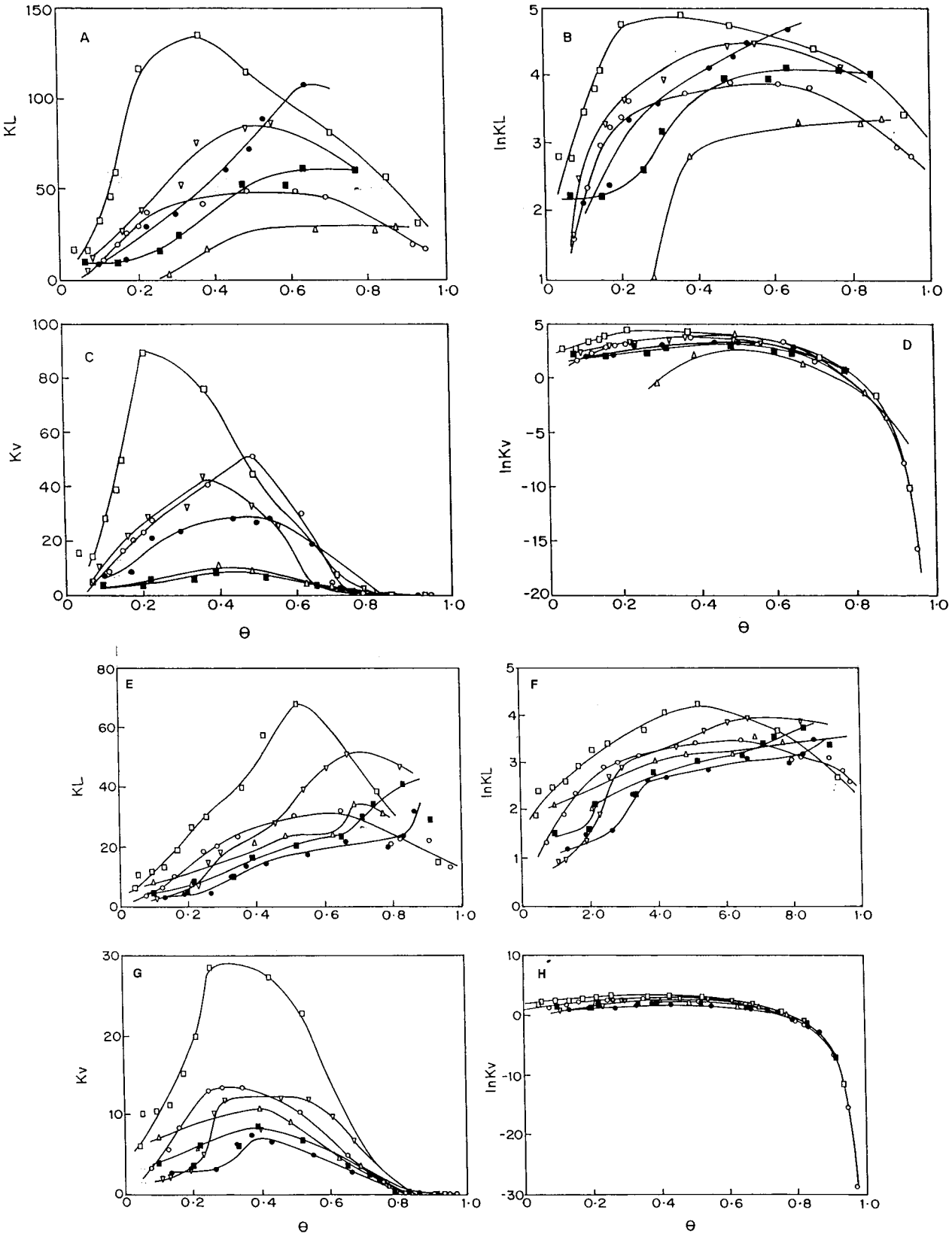

Figure 7. Plots of K_L, ln K_L, K_V, and ln K_V with coverage θ in (A−D) $ALPO_4$-11 and (E−H) MnAPO-11 at (○) 333, (□) 363, (▽) 393, (●) 423, (■) 453, and (△) 483 K.

3.5. Applications of Statistical Models of Langmuir and Volmer. The statistical model equations of Langmuir and Volmer[21] derived initially for ideal systems are often applied to real systems to yield information on the extent of deviation occurring in such systems due to surface heterogeneity, multilayer formation, and mutual interactions between sorbed molecules. The simplest isotherm equation describing localized sorbed molecules on the sites which are independent of each other and are energetically equivalent is that of Langmuir, expressed as follows:

$$P = K_L(\theta/1 - \theta) \qquad (2)$$

TABLE 4. Tests of Isotherm Equations

isotherm equation	plot against θ	result if the model is applicable
(i) $p = K_L(\theta/1-\theta)$	$p(1-\theta/\theta) = K_L$	K_L is independent of θ
(ii) $p = K_{BW}(\theta/1-\theta)\exp(b\theta)$	$\ln p(1-\theta/\theta) = \ln K_L$	straight line with slope $= b$ and intercept $= \ln K_{BW}$
(iii) $p = K_V(\theta/1-\theta)\exp(\theta/1-\theta)$	$p(1-\theta/\theta)\exp(-\theta/1-\theta) = K_V$	K_V is independent of θ
(iv) $p = K_{VW}(\theta/1-\theta)\exp(\theta/1-\theta-\alpha\theta)$	$\ln p(1-\theta/\theta)\exp(-\theta/1-\theta) = \ln K_V$	straight line with slope $= -\alpha$ and slope $= \ln K_{VW}$

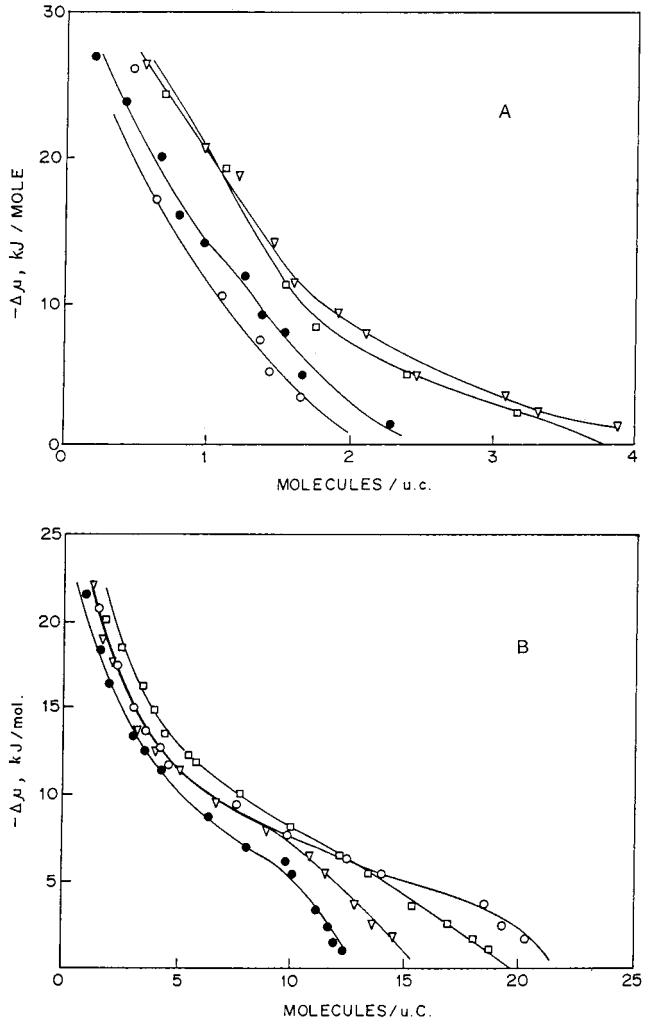

Figure 8. Chemical affinity for ammonia sorption at (A) 483 K and (B) 333 K in (○) $ALPO_4$-11, (□) SAPO-11, (▽) CoAPO-11, and (●) MnAPO-11.

Modified forms of the Langmuir equation have been used[11,18,22,23] to explain the physical properties of the sorbed phase. The resulting equations and methods of testing them are summarized[22,23] in Table 4. The coverage θ was calculated by dividing the amount sorbed at a given pressure by a saturation sorption capacity obtained from the reciprocal of the slopes of P/V against P.

Figure 7 shows the typical plots of K_L, $\ln K_L$, K_V, and $\ln K_V$. K_L plots approximate to linearity but with some $+ve$ slope up to a coverage of 0.6−0.7. Typical $\ln K_L$ plots from Figure 7 show a nonlinear increase up to $\theta = 0.6-0.7$, after which they show a descending curve. There seems the indication of mobile sorption without sorbate−sorbate interaction at lower coverage but mobile sorption with sorbate−sorbate interaction at higher coverage. In conclusion, the ammonia sorption in these phosphate-containing molecular sieves follows localized sorption with sorbate−sorbate interaction and mobile sorption without sorbate−sorbate interaction at low coverage (up to $\theta = 0.6-0.7$). At higher coverage, mobile sorption with sorbate−sorbate interaction is more predominant.

TABLE 5. Isosteric Heats (Q_{st}, kJ mol^{-1}) of Ammonia Sorption

	ammonia molecules/unit cell			
sample	3.00	4.00	5.00	6.00
ALPO-11	30.2	29.6	30.5	30.5
SAPO-11	47.3	40.2	37.4	37.0
CoAPO-11	30.3	29.4	30.0	31.6
MnAPO-11	30.9	29.3	30.1	32.3

3.6. Chemical Affinity and the Selectivity of a Sorbed Phase. When a gas is transferred reversibly and isothermally from the gas phase at a standard pressure P_0 into an infinite amount of sorbate−sorbent mixture over which the equilibrium pressure is P, there is a decrease in the potential. Neglecting the nonideality of the sorbate, the chemical affinity can be expressed[20] as

$$\Delta\mu = RT\ln(P/P_0) \tag{3}$$

The value of $\Delta\mu$ may be taken as the quantitative measure of the chemical affinity of the sorbate for the sorbent. The plots of $-\Delta\mu$ against the amount sorbed also serve as useful criteria for the comparison of sorption affinities of probe molecules in the frameworks of various phosphate-containing molecular sieves having AEL topology.

The typical chemical plots for NH_3 sorption in different phosphate-containing molecular sieves having AEL topology are shown in Figure 8. These plots indicate a slower decrease in the chemical affinity ($-\Delta\mu$) at lower temperature and a sharper decrease in $-\Delta\mu$ at lower coverage than that at higher coverage. At 483 K, the $-\Delta\mu$ at a fixed coverage follows the sequence CoAPO-11 > SAPO-11 > MnAPO-11 > ALPO-11. At 333 K, the sequence in $-\Delta\mu$ at higher coverage become rather complicated following the sequence SAPO-11 > ALPO-11 > CoAPO-11 > MnAPO-11.

3.7. Isosteric Heat (Q_{st}) of NH_3 Sorption. The isosteric heat (Q_{st}) of ammonia sorption is derived by applying the Clausius Clapeyron equation at constant sorbate loadings.[21]

$$Q_{st} = R[(T_2T_1)/(T_2 - T_1)]\ln(P_2/P_1) \tag{4}$$

Table 5 lists the values of the isosteric heats for the sorbate loading ranging from 3 to 6 ammonia molecules/unit cell. The Q_{st} values in the midcoverage region are a result of both sorbate−sorbent and sorbent−sorbent interactions, and depending upon the extent of contribution from each of them, many times humps in the Q_{st} curves are observed.[22] The Q_{st} data tabulated in Table 5 indicated a drop in the isosteric heat at the coverage of 4 molecules/unit cell for all the samples. However, the extent of the drop is (~15%) maximum in the case of SAPO-11. On the basis of the extent of the drop in isosteric heat at the coverage of 4 molecules/unit cell, the samples have shown the following trend SAPO-11 > MnAPO-11 > CoAPO-11 > AlPO-11, which is in accordance with the sequence observed in the hydrophilicity. Similarly, at constant coverage, the Q_{st}

value has shown a similar trend, suggesting the major contribution due to sorbate−sorbent interaction in all the samples.

4. Conclusions

An increase in the hydrophilicity in the Si, Co, and Mn analogues has been demonstrated by the generation of the Bronsted acidity on account of the extent of substitution and the characteristics of the substituent cation. Sorption uptake of *n*-hexane and cyclohexane in ALPO-11 is more than that of its Si, Co, and Mn analogues.

Ammonia sorption isotherms in ALPO-11 and the Si, Co, and Mn analogues of ALPO-11 up to 500 Torr in the temperature range 333−483 K were found to be of Langmuir type. The amount of irreversibly retained ammonia was found to be dependent on the total amount sorbed and on the intrinsic acidity associated with the zeolite framework. The protons generated by the substitution of Co^{2+} or Mn^{2+} in place of Al^{3+} were found to be stronger than the protons generated by the substitution of Si^{4+} in place of P^{5+}.

The saturation capacities obtained from linear Dubinin plots and monolayer capacities obtained from linear Langmuir plots were in close agreement with the sorption capacities obtained experimentally. The affinity coefficient, β, follows the sequence SAPO-11 > MnAPO-11 > CoAPO-11 >ALPO-11, which seems to bear some relation to the expected acidity induced on the silicon or metal substitution in ALPO-11. The statistical model equations of Langmuir and Volmer showed only marginal applicability in ammonia sorption data in AEL-type phosphate-containing molecular sieves and thus did not give very useful information on the state of the sorbed phase. Chemical affinity plots indicate a slower decrease in the chemical affinity at lower temperature and a sharper decrease at higher temperature. The hydrophilicity and the isosteric heat at the coverage of 4 molecules/unit cell has shown the trend SAPO-11 > MnAPO-11 > CoAPO-11 > ALPO-11.

Acknowledgment. The authors are grateful to Dr. P. Ratnasamy, Director, National Chemical Laboratory, for continuous support and encouragement.

References and Notes

(1) (a) Wilson, S. T.; Lok, B. M.; Flanigen, E. M. U.S. Patent 4,310,-440, 1982. (b) Lok, B. M.; Messina, C. A.; Patton, R. L.; Gajek, R. T.; Cannan, T. R.; Flanigen, E. M. U.S. Patent 4,440,871, 1984.

(2) (a) Bennett, J. M.; Richardson, J. W., Jr.; Pluth, J. J.; Smith, J. V. *Zeolites* **1987**, *7*, 160. (b) Richardson, J. W., Jr.; Pluth, J. J.; Smith, J. V. *Acta Crystallogr*. **1988**, *B44*, 367.

(3) (a) Vanoppen, D. L.; DeVos, D. E.; Genet, M. J.; Rouxhet, P. G.; Jacobs, P. A. *Angew. Chem., Int. Ed. Engl*. **1995**, *34*, 560. (b) Chen, J. D.; Sheldon, R. A. *J. Catal*. **1995**, *154*, 1.

(4) Vedrine, J. C.; Coudurier, G.; Mentzen, B. F. *ACS Symp. Ser*. **1988**, *368*, 66.

(5) (a) Flanigen, E. M.; Lok, B. M.; Patton, R. L.; Wilson, S. T. *Stud. Surf. Sci. Catal*. **1986**, *28*, 103. (b) Flanigen, E. M.; Patton, R. L.; Wilson, S. T. *Stud. Surf. Sci. Catal*. **1988**, *37*, 13.

(6) Singh, P. S.; Kosuge, K.; Ramaswamy, V.; Rao, B. S. *Appl. Catal.* **1999**, 177, 149.

(7) Shiralkar, V. P.; Kulkarni, S. B. *Z. Phys. Chem. (Liepzig)* **1983**, *265*, 313.

(8) (a) Singh, P. S.; Bandyopadhyay, R.; Rao, B. S. *J. Chem. Soc., Faraday Trans*. **1996**, *92* (11), 2017. (b) Singh, P. S.; Bandyopadhyay, R.; Shaikh, R. A.; Rao, B. S. *Stud. Surf. Sci. Catal*. **1995**, *97*, 343.

(9) (a) Flanigen, E. M.; Lok, B. M.; Patton, R. L.; Wilson, S. T. EP Patent 158,976, 1986. (b) Wilson, S. T.; Flanigen, E. M. U.S. Patent 4,-567,029, 1986. (c) Chen, J. D.; Lampus, H. E. B.; Sheldon, R. A. *J. Chem. Soc., Faraday Trans*. **1996**, *92* (10), 1807.

(10) Kieselev, A. V. *Discuss Faraday Soc*. **1965**, *40*, 205.

(11) Coughlan, B.; McEntee, J. J. *Proc. R. Ir. Acad.* **1976**, *76B*, 473.

(12) Shiralkar, V. P.; Kulkarni, S. B. *J. Colloid Interface Sci*. **1985**, *108* (1), 1.

(13) (a) Coughlan, B.; McCann, W. A. *J. Chem. Soc., Faraday Trans. 1* **1969**, *75*, 1969. (b) Coughlan, B.; Larkin, P. M. *Chem. Ind*. **1976**, 275.

(14) Rao, G. N.; Joshi, P. N.; Kotasthane, A. N.; Shiralkar, V. P. *J. Phys. Chem.* **1990**, *94*, 8889.

(15) Kulkarni, S. J.; Kulkarni, S. B. *Indian J. Chem*. **1989**, *28A*, 6.

(16) Shiralkar, V. P.; Kulkarni, S. B. *Zeolites* **1984**, *4*, 330.

(17) Joshi, P. N.; Eapen, M. J.; Shiralkar, V. P. *J. Chem. Soc., Faraday Trans.* **1994**, *90* (2), 387.

(18) (a) Shiralkar, V. P.; Kulkarni, S. B. *J. Colloid Interface Sci*. **1986**, *109*, 115. (b) Joshi, P. N.; Shiralkar, V. P. *J. Phys. Chem*. **1993**, *97*, 619.

(19) Dubinin, M. M.; Radushkevich, L. V. *Proc. Acad. Sci., USSR* **1974**, *55*, 327.

(20) Shiralkar, V. P.; Kulkarni, S. B. *Zeolites* **1985**, *5*, 37.

(21) Barrer, R. M.; Coughlan, B. *Molecular Sieves, Soc. Chem. Ind. (London)* **1968**, *141*, 233, 241.

(22) Coughlan, B.; Kilmartin, S. *J. Chem. Soc., Faraday Trans. 1* **1975**, *71*, 1809, 1818.

(23) Coughlan, B.; Shaw, R. G. *Proc. R. Ir. Acad.* **1976**, *76B*, 191.